Modelling the Transport of Corrosion Products and Radionuclides in the CANDU Primary Heat Transport System

O.Y. Palazhchenko[1] **and D.H. Lister**[1]
[1]University of New Brunswick, New Brunswick, Canada
opalazhc@unb.ca

Abstract

An accurate prediction of FAC in a typical CANDU-6 is important for determining radiation fields around components. The current model calculates FAC rates and the transport of non-radioactive and irradiated corrosion products around the primary side. One EFPY of operation is simulated for low- and high- chromium carbon steel. Predictions of corrosion rates in the feeders and deposit accumulation are in good agreement with plant measurements. Activities of ^{59}Fe, ^{55}Fe, ^{58}Co, and ^{63}Ni are obtained from the predicted deposit mass per unit area. On-going work involves modelling surface activity levels resulting from ^{54}Mn, ^{65}Zn, ^{51}Cr, and ^{60}Co transport.

1. Introduction

Transporting heavy water coolant to and from the fuel channels, the inlet and outlet headers and feeder pipes are an integral part of the CANDU primary heat transport system (PHTS). With the formation of generally corrosion-resistant layers under PHTS conditions [1,2], carbon steel (CS) and nickel alloys such as the Alloy-800 of steam generator (SG) tubing are commonly-used materials. However, degradation of CS outlet feeders attributed to flow-accelerated corrosion (FAC) was reported at the Point Lepreau Generating Station (PLGS) in the mid-1990s, followed by similar observations at other CANDU plants.

FAC results in feeder degradation, accumulation of particulate oxide (crud) on the fuel and steam generators, and transport and irradiation of corrosion products. Soluble and particulate species traversing the reactor core undergo neutron activation, generating gamma- and beta-emitting isotopes. A model devised by Atomic Energy Canada Limited (AECL) [3], following earlier studies [4], proposes proportionality between surface activity and oxide deposition. Thus, an accurate prediction of film loading with time is necessary.

A comprehensive computer program that includes kinetics, mass transfer, electrochemistry, and erosion for both steel and nickel alloy surfaces has been developed. This paper outlines the model, focusing on the surface activities of radionuclides derived from Ni and Fe parent isotopes and lays groundwork for modelling nuclides resulting from PHTS impurities.

2. Modelling

A general corroding surface and the pertinent processes are shown in Figure 1. The growth of the inner and outer oxides occurs at the metal-oxide and solution-oxide interfaces (M/O and S/O, respectively). At the M/O, metal ions not contributing to the inner layer diffuse through it to the S/O, where either growth of the outer layer or transport to the bulk coolant takes place. The *in-situ* oxide films modelled on system surfaces are shown in Table 1, which indicates two feeder compositions.

Table 1 *In-situ* oxide compositions on PHTS surfaces.

Layer	0.019 wt% Cr CS	0.33 wt% Cr CS	Alloy-800
Passivating	N/A	$FeCr_2O_4$	N/A
Inner	Fe_3O_4	*$Fe_{3-x}Cr_xO_4$	$FeCr_2O_4 + Ni_{0.6}Fe_{2.4}O_4$
Outer	Fe_3O_4	Fe_3O_4	$Ni_{0.6}Fe_{2.4}O_4 + Ni$

*x<0.001, having a very small effect on diffusion

In light of the fact that increasing the Cr content from 0.019 to 0.2-0.4 wt% reduces the FAC rate of CS [5], 0.33 wt% Cr steel, representative of the replacement feeders at PLGS, is also modelled. The corrosion mechanism involves a very thin, chromium-rich "passivating" layer, possibly $FeCr_2O_4$, beneath the Fe_3O_4 at the metal-passivating-layer (M/P) interface [6].

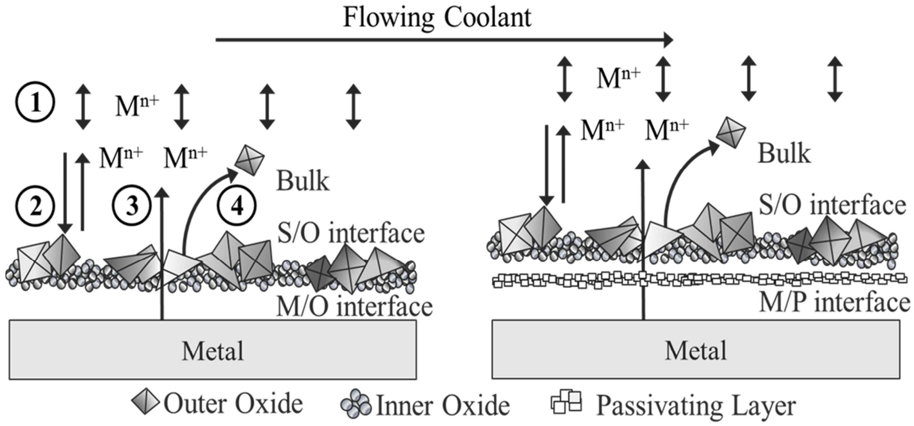

Figure 1 General metal surface (left) and steel with passivating layer (right).
1. Mass transfer, 2. Precipitation/dissolution, 3. Diffusion, 4. Erosion.

2.1 Overall Computation

The general model is a development of the work of Lister and Lang [7], Cook et al. [10], and Silpsrikul [11]. The central calculation is based on the fourth-order Runge-Kutta method, where oxide thickness is determined from the weighted average of four approximations along a time step. As the thickness is contingent on corrosion rate, the procedure is iterative.

The dominant radionuclides in the PHTS include: ^{58}Co, ^{60}Co, ^{51}Cr, ^{59}Fe, ^{55}Fe, ^{65}Zn, ^{54}Mn, and ^{63}Ni. It is postulated that activity accumulates in the outer oxide layer *via* direct surface precipitation, *via* diffusion into the oxide through pores followed by incorporation, or *via* a combination of the two. The AECL empirical observation that ^{60}Co activity is proportional to surface Fe_3O_4 accumulation is extended to the oxides (Table 1) and isotopes examined here. This follows the original theory of Lister [4]. The specific activity calculation is performed analogously to that of Guzonas and Qui [3] and used alongside deposit mass to determine the surface activity of each radionuclide.

3. Results

3.1 Material and Activity Transport

The oxide loadings around the PHTS after 1 EFPY are presented in Figure 2a. A high velocity (16.19 m/s) outlet feeder is modelled. As expected, the corrosion of the outlet feeder nodes, averaging103 µm/a, is higher than that of the inlet (4.5 µm/a). The high outlet feeder velocity promotes erosion, which affects the inner oxide surface once the outer film is no longer available.

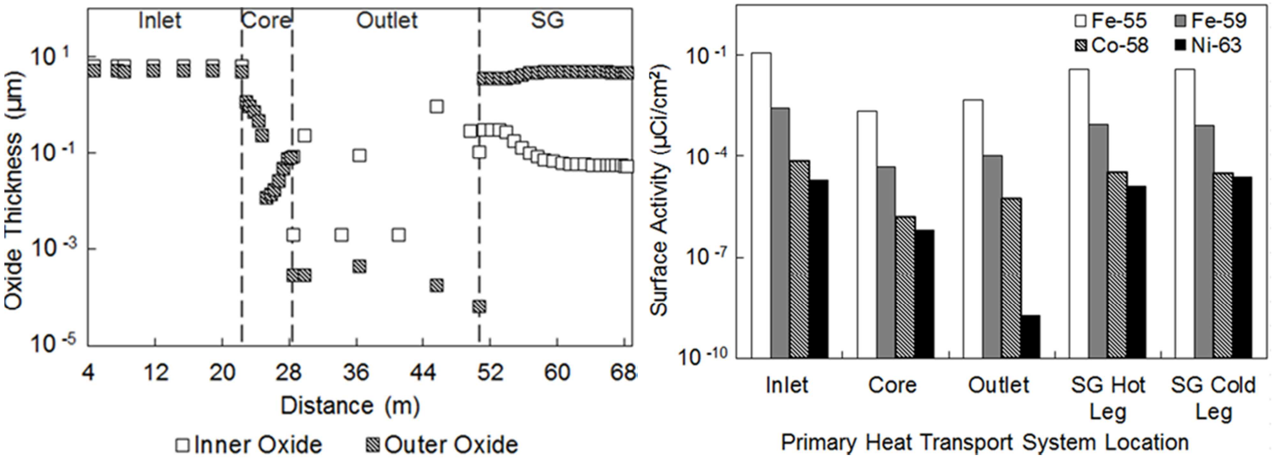

Figure 2 (a) Corrosion rate (left) and (b) radionuclide spatial distribution in the PHTS (low-Cr CS).

Table 2 Average steam generator loadings per EFPY.

Data Source	Hot Leg (mg/cm^2)	Cold Leg (mg/cm^2)
This Model	1.8	2.6
Bruce B (Unit 5) [8]	0.875	2.75
Gentilly-2 [12]	0.43 ± 0.12	1.57-2.49 ± 0.63

A thickness of 3.3 µm at the SG hot leg entrance and a cold leg accumulation of 4.8 µm translate to loadings of 1.8 mg/cm^2 and 2.6 mg/cm^2, respectively. As generally occurs in practice, accumulation begins on the hot leg and increases on the cold side as the coolant supersaturates [8,12]. Assuming that the growth rate reaches steady state by 1 EFPY, outer layer data from Bruce B is interpolated to a minimum 0.875 mg/cm^2 and maximum 2.75 mg/cm^2 after 1 EFPY on the cold and hot sides, respectively, which is in good agreement with our predictions as presented in Table 2.

Figure 2b shows the activities around the PHTS, where radionuclide concentration is high in the inlet and SG. This is in agreement with station reports that show radioisotope build-up mirrors oxide accumulation, particularly in the SG cold leg [3,13]. The $Ni_{0.6}Fe_{2.4}O_4$ and Fe_3O_4 deposits are assumed to be the primary sinks for the iron radionuclides, while ^{63}Ni accumulation is considered predominantly in nickel ferrite and metallic Ni. ^{58}Co is expected to preferentially incorporate into the tetrahedral sites of the normal spinel $FeCr_2O_4$ *versus* the inverse spinel Fe_3O_4 and $Ni_{0.6}Fe_{2.4}O_4$ lattices. This is accounted for *via* a ratio of the stabilization energies of Co^{2+} in these spinels [9].

3.2 High *versus* Low Chromium Content

The predicted corrosion rates of the high- and low-Cr CS are shown in Figure 3. The decrease in the degradation ranges from about 40 to 50% along the outlet feeder, with average rates of 55 µm/a *versus* the 103 µm/a for the low-Cr CS. The predicted effect of chromium is consistent with plant observations, where reductions of FAC rates of 50% or more have been measured [14]. No major difference is seen in the inlet feeders, where corrosion is relatively slow.

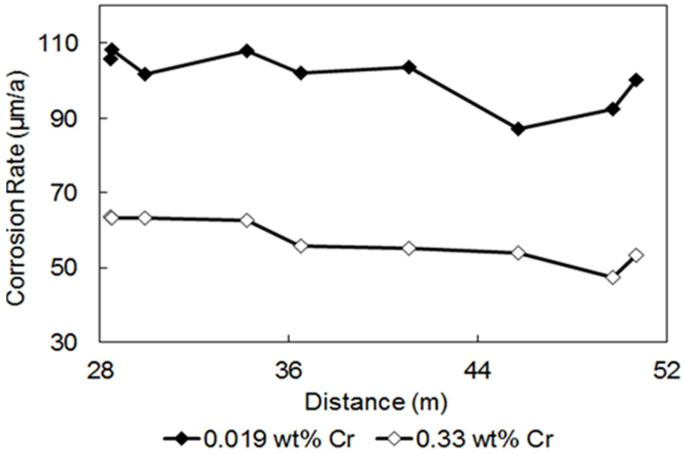

Figure 3 High velocity outlet feeder corrosion rate for low- and high-Cr content CS.

4. Conclusions

The transport of Fe and Ni due to FAC and general corrosion alongside neutron activation and transport have been successfully modelled for the CANDU 6 PHTS. Overall, the results are within the ranges of station data; however, it is noted that the reactor types are not all CANDU 6s with Alloy 800 SG tubes. The modelling of by-products of SG tubing corrosion could be improved if more kinetic precipitation and dissolution data were available. Modelling of ^{60}Co, ^{65}Zn, ^{51}Cr, and ^{54}Mn transport is under development.

5. References

[1] Potter, E.C., Mann, G.M.W., "Oxidation of mild steel in high-temperature aqueous systems," First International Conference on Metallic Corrosion, London, UK, 1962.

[2] Alvarez, M.G., Olmedo, A.M., "Corrosion behaviour of alloy-800 in high temperature aqueous solutions: long term autoclave studies," Journal of Nuclear Materials, Vol.29, 1996, pp.93-101.

[3] Guzonas, D.A., Qui, L., "Modeling activity transport in the CANDU heat transport system," Nuclear Plant Chemistry Conference, Quebec, Canada, October 3-7, 2010.

[4] Lister, D.H., "The transport of radioactive corrosion products in high temperature water II. The activation of isothermal steel surfaces," Journal of Nuclear Science and Engineering, Vol.59, 1976, pp.406-426.

[5] Tapping, R.L., “Corrosion issues in pressurized heavy water reactor (PHWR/CANDU) systems,” Nuclear corrosion science and engineering, Feron, D. (Ed.)., Woodhead Publishing, Cambridge, UK, pp.104, 2012.

[6] Phromwong, P., et al., “Modelling material effects in flow-accelerated corrosion,” International Conference of Environmental Degradation of Materials in Nuclear Power Systems, Colorado, USA, August 6-11, 2011.

[7] Lang, L., Lister, D.H., “A mechanistic model for predicting flow-assisted and general corrosion of carbon steel in reactor primary coolants,” International Conference of Water Chemistry in Nuclear Reactor Systems, Avignon, France, April 22-26, 2002.

[8] Guzonas, D.A., Qui, L., “A predictive model for radionuclide deposition around the CANDU heat transport system,” International Conference on Water Chemistry of Nuclear Reactor Systems, San Francisco, USA, October, 2004.

[9] Lister, D.H., “Activity transport and corrosion processes in PWRs,” Journal of Nuclear Energy, Vol.32, Iss.2, 1993, pp.103-114.

[10] Cook, W.G., Lister, D.H., and McInerney, J.M., “The effects of high liquid velocity and coolant chemistry on material transport in PWR coolants,” 8th Water Chemistry of Nuclear Reactor Systems Conference, Bournemouth, UK, BNES, October 22-26.

[11] Silpsrikul, O., “Modelling of corrosion and iron transport in the primary heat transport system of CANDU reactors,” Ph.D. Thesis, University of New Brunswick, 2007.

[12] Semmler, J., Allen, J.L., “Analysis of steam generator tube sections removed from Gentilly-2 nuclear generating station” Nuclear Plant Chemistry Conference, Quebec, Canada, October 3-7, 2010.

[13] Lovasic, M., Upton, M., “Activity balance in Ontario hydro primary heat transport system as information for radioactive management,” Waste Management Conference, Tucson, USA, February 28-March 4, 1999.

[14] Slade, J., Gendron, T., “Flow accelerated corrosion cracking of carbon steel piping in primary water -operating experience at Point Lepreau Generating Station,” 12th International Conference of Environmental Degradation of Materials in Nuclear Power Systems, Utah, USA, August 14-18, 2005.